Heron's fountain 18

Finds and ideas with a surprising element similar to the playful inventions of Heron of Alexandria, after whom this journal is named

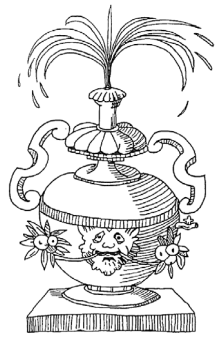

200 Years old Cauchy concept pointed the route to optimizing concrete porosimetry in virtual reality

The solution of a technical problem is in many cases potentially available however probably somewhat hidden in the literature. At least, research engineers in concrete technology have the tendency not to search for it but to come up with their own ideas. Unfortunately, not always of the same standard as guaranteed by the original source. Interestingly, many powerful theoretical concepts relevant for concrete technology are of stereological nature, although in many cases (much) older than stereology itself (Stroeven and Hu, 2006; Stroeven *et al.*, 2009). With the development of stereology as a science since the foundation of the society for stereology in 1963, old roots became apparent: stereology *avant la lettre*. As a concrete technologist the second author of this fountain enjoyed several *playful discoveries* over the years that in some cases constituted old but reliable milestones along the route to solving popular problems in our field. Baron Augustin-Louis Cauchy (21 August 1789 – 23 May 1857) formed such a milestone. He was a French mathematician reputed as a pioneer of analysis. He was one of the first to state and prove theorems of calculus rigorously. Of the extensive oeuvre of Cauchy, two formulas – almost two centuries old – are of significance for concrete technology (and other branches of science) (Cauchy, 1882; Stroeven and Hu, 2006)

$$L = \tfrac{1}{2}\pi\,\overline{L}' \tag{1}$$

$$S = 2\overline{A}' \tag{2}$$

Eq. (1) states that the length of an artificially curved line in a plane, L, equals $\pi/2$ times the average value of its total projected length, L', in a series of random or systematic directions (Fig. 2). Eq. (1) found interesting applications for the orientation and effciency of fibres in

concrete (Stroeven, 1977; Stroeven, 2015). Noteworthy is that also here geometric avaraging proofed difficult (Romualdi and Mandel, 1964; Souroushian and Lee, 1990).
Eq. (2) states that the surface area of an artificially curved element in space, S, equals 2 times the average value of its total projected area, A', in a series of randomly or systematicly oriented planes. Eqs. (1) and (2) were earlier used for the analysis of damage in concrete (Stroeven, 1979; 2000).

Figure 1. Cauchy around 1840. Lithography by Zéphirin Belliard after a painting by Jean Roller (source: Wikipedia)

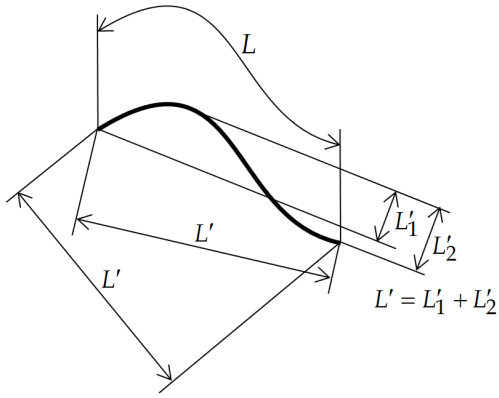

Figure 2. Illustration of Equation (1) L is the length of a curved line, L' stands for its total projected length.

1 Global geometric averaging

Before we will enter the complicated field of permeability estimation, we first proof that Eq. (1) is correct for a straight fiber. Figure 3 shows this fiber with a length L. It is projected onto a line with angle θ. This angle can have any value between 0 and π. The projection has the length $L' = L|\cos\theta|$. The average $\bar{L}'$ of all L' is the integral over all θ divided by π.

$$\bar{L}' = \frac{\int_0^{\pi} L|\cos\theta|\, d\theta}{\pi} = \frac{2}{\pi}L \tag{3}$$

We now proof that Eq. (2) is correct for a sphere. A sphere has a surface area $S = 4\pi r^2$. The total projection of this sphere on a plane is $A' = \pi r^2 + \pi r^2$. Hence, both top and

bottom sides of the sphere are accounted for in the projection plane. Since all projections are similar, the average $\bar{A}'$ of all possible projections is equal to A'. Consequently,

$$\frac{S}{\bar{A}'} = 2 \tag{4}$$

Hence, for a straight fiber and a sphere the derivation of Eqs. (1) and (2) is relatively simple.

Subsequently, we use the Cauchy principles in Eq. (2) to deal with dispersed surfaces that enclose pore space. For this global averaging operation (required to go from micro-level to the engineering one), we can use a unit sphere model as presented in Fig. 4. The surfaces in space can be subdivided into small, flat elements, ΔS, that can be translated towards the unit sphere so that they touch this unit sphere's surface. The projection A' on the horizontal plane is

$$A' = S\frac{\int_0^{\pi/2} \sin\theta\cos\theta \, d\theta}{\int_0^{\pi/2} \sin\theta \, d\theta} = \frac{1}{2}S \tag{5}$$

The 3D situation of global geometric averaging has in concrete technology practice resulted in quite some confusion. What we will consider next is a case of global geometric averaging of pore microstructure in hardened *virtual* cement paste.

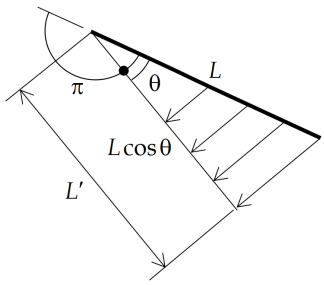

Figure 3. Straight fiber projected on a line

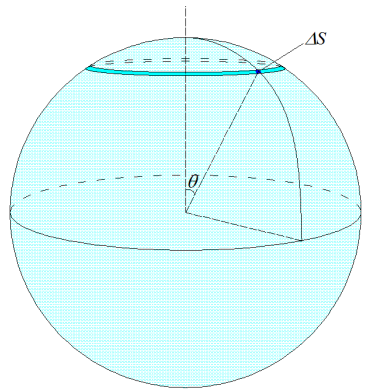

Figure 4. Unit sphere with infinitely small surface element ΔS (from a crack or pore) attached to it

2 Generation of pore microstructure in virtual cement paste

The details of the generation of pore microstructure are described in the international literature (Stroeven *et al.*, 2012; Le, 2015). Here we will just present a survey, so that the reader can imagine what has to be done. In the first place, the cement is modelled by a range of spherical particles with a specified (Rosin-Rammler type) size distribution. Next, the virtual cement is packed by a discrete element method (HADES) in a cubic container. To do so, the container is enlarged and the spherical particles dispersed in it by a random generator. Next, the particles are set to linearly move and collide mutually and with the surfaces of the container, which is gradually reduced to the desired size. When this dynamic stage is terminated, the particle mixture has its required density, so that the addition of water leads to the objected *w/c* ratio.

The cement particle packing is thereupon hydrated with the advanced hydration simulation package XIPKM (Le *et al.*, 2013). This leads to complicated interferences of cement particles expanding by the deposition of CSH at their free surface. The remaining phase is pore space that is reduced by the hydrating particles. Further, pore continuity is reduced by depercolation. Finally, DRaMuTS (Stroeven *et al.*, 2012) is applied as an improved version of the rapidly-exploring random tree (RRT) procedure in robotics. It imaginary involves large numbers of infinitely small robots to find their way from surface-to-surface through the cubic specimen. The result is a multiple tree-like structure of zig-zag-shaped routes (Fig. 5, left). Removal of the dead-end braches and isolated pores yields the continuous channels (Fig. 5, right). The zig-zag lines in the main channels are finally smoothed by mathematical techniques. Hence, full topology of the pore network structure is known, only the pore size distribution function, required for permeability assessment, is missing. For the latter purpose, a system of about 10^5 points is dispersed in pore space whereupon pore size is assessed in all points by star volume measuring, SVM (Stroeven *et al.*, 2010). This involves having a series of randomly or systematically oriented pikes running from the point to the pore surface. These pikes l_j are measured per point i and used in Eq. (6)

$$d_i = 2\sqrt[3]{\overline{l_j^3}} \tag{6}$$

whereby d_i is the diameter of the local representative sphere. All these local pore size measures are used for constructing a volume-based pore size distribution function, PoSD. This could be used as input for the pore network model. Yet, for fluid or gas transport in

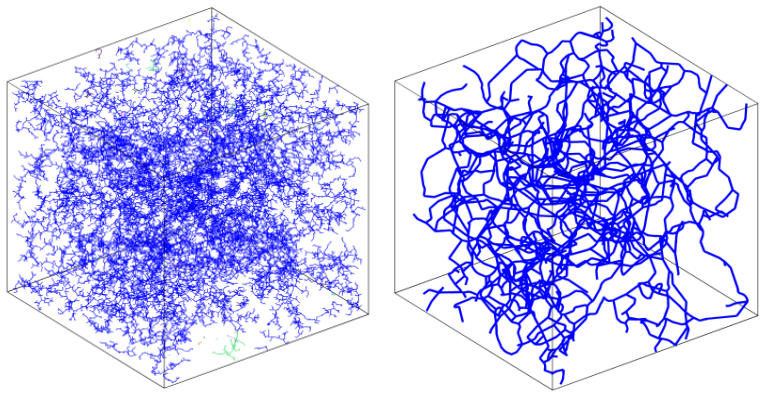

Figure 5. (left) All pores in 90 days hydrated cement paste with w/c = 0.4 and Blaine surface area of 300 m²/kg. Porosity is 19%. (right) Only main pore channels of the same cement paste.

the pores, the diameter of the smallest section was considered a better measure for 'size'. Hence, in all 10^5 points 2D pore sections were considered. They were 'randomly' rotated around all the points, whereby size (of the representative circle) was determined in all cases per point. The section with smallest area was denoted the throat section and used in the pore network model. It rendered possible constructing a throat size distribution function, ToSD. It must be obvious, however, that the process of finding the throat area in all the points is a time-consuming operation. In fact, all successive operations (DEM packing, hydration simulation by XIPKM, pore delineation by DRaMuTS and pore measuring by SVM) required about one hour. The question to be solved herein is whether Cauchy could help us reducing the SVM stage significantly.

3 Playful discovery by Cauchy application to SVM

In search for an easier SVM solution – unaware of Cauchy – Le (2015) tried only using a single IUR pore section per dispersed point. This would offer a dramatic reduction in efforts, of course. The resulting random section size distribution function (TrSD) shifted to somewhat larger pore values than the ToSD, with curves of quite similar shape. Promising was that the ratio of median pore size values of the two curves seemed stable. To find a theoretical basis for this SVM concept, we will apply Cauchy's solution in Eq. (2) for the 'average projected surface area in space' to the pore microstructure case. Note that the standard approach yields throat sizes in 10^5 points. So, these results could be classified in, say, 300 very narrow classes of successive pore sizes. Let's consider such a class of (average) throat size d. This fraction of (almost) mono-size throats is in the short approach

replaced by an IUR set of larger pore sections. When we represent the real throat section by that of its representative circle, the pore neighborhood could be approximated by a cylinder with diameter d (Fig. 6, right). The IUR set of sections in the short approach could be replaced by elliptical sections of the cylinder through the center of the circle, while maintaining their spatial orientation. This completes the Cauchy set up. The area of the throat section is A'. The other sections A_i are projections in the direction of the cylinder axes on a IUR set of planes. So, projecting all IUR sections onto the throat section would imply the average projected section area to be twice the throat area - according to Cauchy (Fig. 6, left). This holds for all 300 classes of throat areas. Hence, the conclusion can be drawn that the average value of the IUR set of section areas would be twice that of the throat area. This Cauchy factor of 2 correlates the two approaches. More common is a comparison in terms of size, which would obviously lead to a correlation factor of √2. This Cauchy solution for SVM is checked for various cases of which the results are plotted in Fig. 7. It depicts the ratio of median size values of pore sections in the standard approach (throats) and in the short one. These data present clear evidence for the reliability of the short method. Cauchy pointed the road to finding such a solution. It reduces the time-consumption to about 15% of that of the standard approach.

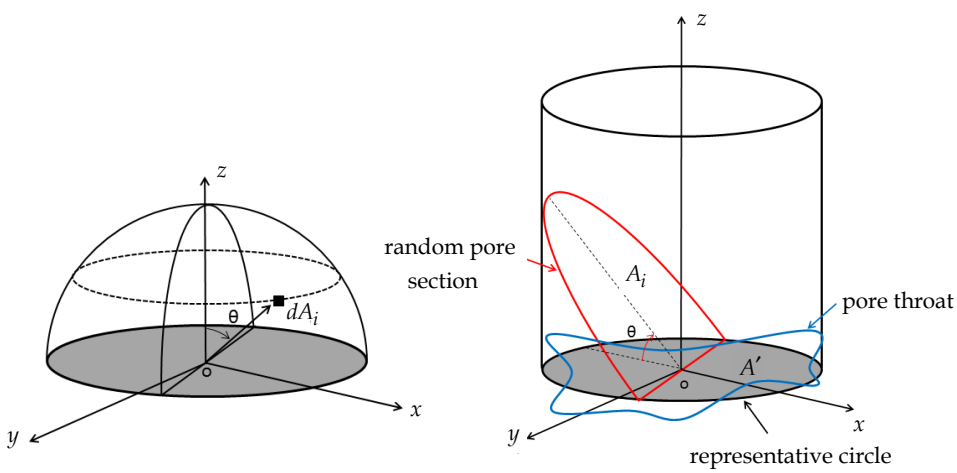

Figure 6. Schematized situation at a throat section in the pore microstructure. The throat is represented by its representative circle of size d and the local pore by a cylinder of equal width. A single randomly oriented pore section from the short approach pertaining to the same throat size is indicated (right). Infinitely small random pore section elements of all random sections pertaining to the same throat size are collected on the surface of the unit sphere (left).

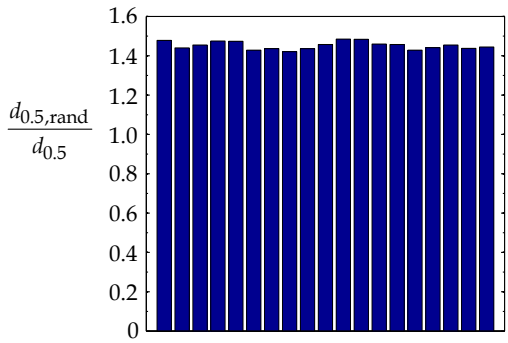

Figure 7. Ratio of median pore size values obtained by the short "random", $d_{0.5,\ rand}$, and by the standard approach, $d_{0.5}$, for 19 different cases. The results fluctuate around the value of $\sqrt{2}$.

4 Discussion and conclusions

Cauchy's formula for projected surfaces in space (although flat in the present case) provided a far more economic route toward the construction of the throat size distribution function. Specifically, it rendered possible realizing about 85% reduction in efforts to be bestowed on the SVM (star volume measuring) stage. So, porosimetry could be promoted by application of a 200 years old concept! Really, a playful discovery.

The discussion on the obtained size of the pores by this analogue method (to be distinguished from a digitized one) has been proven misleading. The permeability of cement paste partially saturated by water (representing relevant engineering conditions) has been proven supported by recently published experimental data obtained by water permeability tests (Stroeven *et al.*, 2015). Traditionally, MIP data are employed for comparison reasons. However, these data are proven significantly biased (Diamond, 2000).

Kai Li [1,2] and P. Stroeven [2]

[1] Key laboratory for Green & Advanced Civil Engineering Materials and Application Technology of Hunan Province, College of Civil Engineering, Hunan University, 410082 Changsha, China

[2] Faculty of Civil Engineering and Geosciences, Delft University of Technology, Stevinweg 1, 2628 CN Delft, the Netherlands

Literature

Cauchy, A. (1882). *Mémoires sur la rectification des courbes et la quadrature des surfaces courbes*. Cambridge Univ. Press, Cambridge, UK (in French)

Diamond, S. (2000). Mercury porosimetry: an inappropriate method for the measurement of pore size distribution in cement-based materials. *Cem. Concr. Res.* 30: 1517-25.

Le, L.B.N., Stroeven, M., Sluys, L.J., Stroeven, P. (2013). A novel numerical multi component model for simulating hydration of cement. *Comp. Mater. Sci.* 78: 12-21.

Le, L.B.N. *Micro-level porosimetry of virtual cementitious materials – Structural impact on mechanical and durability evolution*. Ph.D. thesis, Delft University of Technology, the Netherlands, 2015.

Romualdi, J.P., Mandel, J.A. (1964). Tensile strength of concrete affected by uniformly distributed and closely spaced short lengths of wire reinforcement. *ACI J. Proc.* 61: 657-671.

Souroushian, P., Lee, C-D. (1990). Distribution and orientation of fibers in steel fiber reinforced concrete. *ACI Mat. J.* 87: 433-439.

Stroeven, P. (1977). The analysis of fibre distributions in fibre reinforced materials. *J. Microsc.* 111: 283-295.

Stroeven, P. (1979). Geometric probability approach to the examination of microcracking in plain concrete. *J. Mat. Sci.* 14: 1141-1151.

Stroeven, P. (2000). A stereological approach to roughness of fracture surfaces and tortuosity of transport paths in concrete. *Cem. Concr. Comp.* 22: 331-341.

Stroeven, P. *Modelling fibre reinforcement. In: 50 years' focus on concrete – from meter- to nano-scale*, Media Center, Rotterdam, the Netherlands, 2015.

Stroeven, P., Hu, J. (2006). Review paper – stereology: Historical perspective and applicability to concrete technology. *Mat. Struct.* 39: 127-135.

Stroeven, P., Hu, J. and Guo, Z. (2009). Shape assessment of particles in concrete technology: 2D image analysis and 3D stereological extrapolation. *Cem. Concr. Compos.* 31: 84-91.

Stroeven, P., Hu, J., Koleva, D.A. (2010). Concrete porosimetry: Aspects of feasibility, reliability and economy. *Cem. Concr. Compos.* 32: 291-99.

Stroeven, P., Le, L.B.N., Sluys, L.J., He, H. (2012). Porosimetry by double random multiple tree structuring. *Image Anal. Stereol.* 31: 55-63.

Stroeven, P., Li, K., Le, L.B.N., He, H., Stroeven, M. (2015). Capabilities for property assessment on different levels of the micro-structure of DEM- simulated cementitious materials. *Constr. Build. Mater.* 88: 105-117.

Stroeven, P., Li, K. (2017). A modern approach to porosimetry of virtual cementitious materials. *Mag. Concr. Res.* 69(23): 1212-1217.

Note that Stroeven and Li (2017) is an elaboration of this Heron's Fountain particularly focusing on the engineering results. It was submitted to Mag. Concr. Res. about a year later than the present one to Heron. Unfortunately, the publication date in Heron significantly exceeds the one in Mag. Concr. Res. Hence, no reference could be made in Mag. Concr. Res. to this Heron's Fountain.